Biomacromolecules

pubs.acs.org/Biomac

Article

Thermoplastic "All-Cellulose" Composites with Covalently Attached Carbonized Cellulose

Lotta H. Gustavsson, Karin H. Adolfsson, and Minna Hakkarainen*

Cite This: *Biomacromolecules* 2020, 21, 1752−1761

Read Online

ACCESS | Metrics & More | Article Recommendations | Supporting Information

ABSTRACT: Thermoplastic "all-cellulose" composites were synthesized by covalent functionalization of cellulose acetate (CA) with oxidized carbonized cellulose (OCC). The OCC were manufactured via microwave-assisted hydrothermal carbonization (HTC) of cellulose followed by oxidation and dialysis. The OCC were of micrometer-size, had plane morphology and contained a variety of oxygen functionalities, enabling transformation into acyl chlorinated OCC under moderate reaction conditions. The synthesis of OCC-modified CA composites and neat CA were performed in the recyclable ionic liquid 1-allyl-3-methylimidazolium chloride. The degree of acetylation and amount of OCC were varied to establish their influence on thermal and physical properties of the composites. The OCC-modified CA composites displayed a notably enhanced film-forming ability, which led to improved optical and mechanical properties compared to neat CA. In addition, it was shown that OCC-modified CA composites can be synthesized from waste products, such as paper tissues. The OCC-modification was demonstrated to be a promising route to transparent and strong thermoplastic "all-cellulose" composites with moderate flexibility.

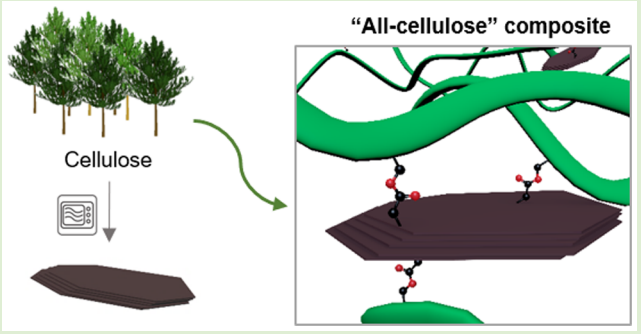

INTRODUCTION

The need for high-quality, biodegradable materials from renewable sources is evident, considering the plastic waste accumulation and the depleting fossil reserves. Cellulose is an appealing candidate for the development of future materials due to its biocompatibility, biodegradability and chemical modifiability.[1−3] However, due to the inherent H-bonding network and the tight fibrous structure of cellulose, it cannot be melt-processed and it is basically nonsoluble in traditional solvents, which have restrained the application of cellulose-based materials.[1,4] Lately, ionic liquids (ILs) that efficiently dissolve cellulose by disrupting the H-bonding[5] have been widely applied for cellulose modification and processing.[2,3,6−9]

Cellulose acetate (CA) is a semisynthetic, biocompatible derivative of cellulose produced through acetylation of the hydroxyl groups on cellulose.[6,10] Acetylation leads to the emergence of thermoplastic properties, although CAs remain difficult to the melt-process due to the small temperature window between the glass transition (T_g) and degradation temperatures.[2,11] The properties of CA, such as solubility[3,10] and biodegradability,[12−14] are largely affected by the degree of substitution (DS).[11,15,16] CA is not a particularly strong material and it yields brittle films,[17] which is why it needs to be modified with plasticizers and other components to produce stronger and more ductile materials.[18−24]

The cellulose-derived carbonized particles, such as oxidized carbonized cellulose (OCC) belong to a group of hydrothermally carbonized materials that have wide potential as functional fillers in various functional composites.[25−27] The carbonized structures can be used as property enhancing fillers in the same way than graphene derivatives,[28−32] clay,[23,33] or lignin particles,[34] which have been shown to increase, for example, the Young's modulus, tensile strength, thermostability, and the gas-barrier properties of cellulose materials.[24,29−31,35] Covalent attachment of fillers provides better longevity for materials as unbound fillers might migrate within or out of the composite matrix.[2]

The hydrothermal carbonization (HTC) is an efficient and green route for production of value-added carbonized materials from low-quality organic matter such as waste paper.[36,37] HTC is typically performed in aqueous solution and at relatively low temperatures (~170−300 °C). Carbonized structures have a content of different oxygen functionalities such as hydroxyl, epoxy and carboxyl groups,[36,37] which further provide attractive options for modification. Our previous studies, where biobased carbonized products were physically blended with, for example, polylactide (PLA),[32,38] polycaprolactone,[38,39] and chitosan,[40] showed enhancement of mechanical strength with sufficient ductility. The PLA nanocomposites also displayed improved barrier properties.[25]

Special Issue: Anselme Payen Award Special Issue

Received: December 5, 2019
Revised: February 9, 2020
Published: February 12, 2020

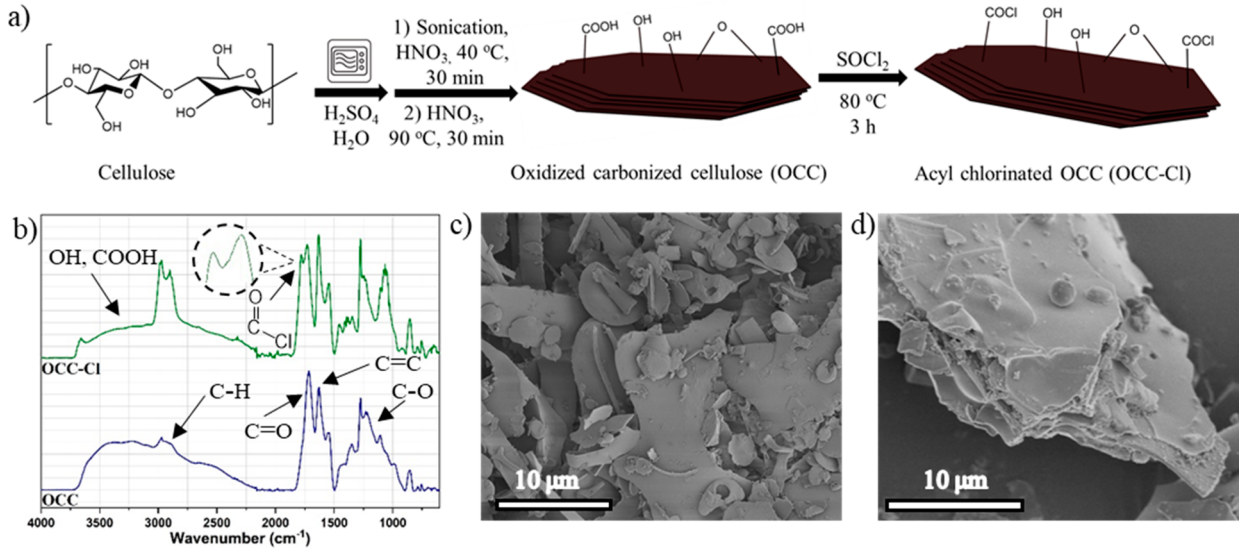

Figure 1. (a) Reaction pathway from cellulose to OCC-Cl. OCC and OCC-Cl are drawn schematically and not in scale. (b) FTIR spectra of OCC and OCC-Cl. (c) SEM image showing the polydispersity of OCC. (d) SEM image showing the layered structure of OCC-Cl.

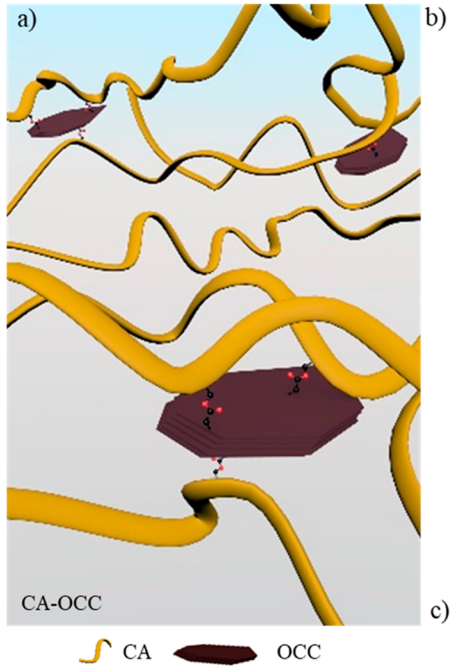

b)

Sample name	DS	OCC (wt-%)	T_g (°C)	Drying method
Cellulose-OCC18	0	18	-	Vacuum
CAL	1.1-1.5	0	186	Vacuum
CAL + 2wt% OCC	1.1-1.5	2	187	-
CAL-OCC2	1.5	2	175	Vacuum
CAL-OCC4	1.1	4	-	Vacuum
CAL-OCC16	0.8	16	-	Fresh (reverse synthesis)
CAH	2.0	0	198	Fresh
CAH(PT)	1.9	0	175	N_2
CAH(PT)-OCC1	2.4	1	185	N_2
CAH-OCC15	2.3	15	187	Fresh

Figure 2. (a) Schematic illustration of CA-OCC composites (not drawn in scale). (b) A table summarizing the sample names with their corresponding DS, amount of OCC, T_g and drying methods (Fresh = freshly synthesized ionic liquid; Vacuum = vacuum at 80−100 °C overnight; N_2 = sweeping with N_2). (c) The appearance of the samples indicating the presence of the OCC in the composite products.

Thermoplastic "all-cellulose" composites with excellent material properties would be appealing materials for a sustainable bioeconomy.[7,41] We hypothesized that covalently attached OCC could improve the mechanical performance of a CA. Covalent CA-OCC composites with varying DS and amount of OCC were therefore synthesized in 1-allyl-3-methylimidazolium chloride (AmimCl), an IL with remarkable solvent properties.[6,9,42] It was further demonstrated that an abundant waste product, paper tissues (PT), could be utilized as a raw material source for the "all-cellulose" composites taking further steps toward a circular resource economy.

EXPERIMENTAL SECTION

Materials and Chemicals. α-Cellulose, thionyl chloride ($SOCl_2$), nitric acid (70%), sulfuric acid (95−98%), acetic anhydride, allyl chloride, and 1-methylimidazolium were purchased from Sigma-Aldrich. The chemicals were of reagent grade. Sodium hydroxide pellets were purchased from Merck. Methanol (MeOH) and dimethyl sulfoxide (DMSO) were of technical grade and purchased from VWR. Ethyl acetate of reagent grade was purchased from VWR. The paper tissues were from Katrin. Allyl chloride was distilled prior use, while the other chemicals were used as received. Deionized water was used in the experiments.

Synthesis of Oxidized Carbonized Cellulose (OCC). Synthesis of OCC was performed according to previously published synthesis

https://dx.doi.org/10.1021/acs.biomac.9b01672
Biomacromolecules 2020, 21, 1752−1761

method through microwave-assisted hydrothermal carbonization of cellulose[36] with some modifications. In a Teflon vessel, 2 g of α-cellulose and 20 mL of 0.1 g/mL H_2SO_4 were added. The carbonization was performed in a flexiWAVE microwave (Milestone Inc.) with the following program: the temperature was raised to 220 °C with a ramp time of 20 min and then kept at 220 °C for 2 h with addition of stirring inside the vessels. The temperature was monitored with a probe inside one of the vessels. After the reaction, the resulting carbonized sample was filtered, washed with water and dried. A total of 1 g of the carbonized sample was further oxidized by sonicating in a round-bottom flask with 100 mL of 70% HNO_3 at 40 °C for 30 min, after which the reaction mixture was refluxed in a heat bath at 90 °C for additional 30 min. The reaction mixture was then poured into 200 mL of H_2O, and the remaining solid particles were removed. The acidic water was evaporated with rotary evaporator until 10−20 mL was left, and the remaining solution was dialyzed against water for 5 days. The final product was dried, and the obtained oxidized carbonized cellulose (OCC) were reddish black in color.

Acyl Chlorination of OCC. The OCC was transformed into OCC-Cl by adding 1 mL of thionyl chloride in a flask with 30 mg of OCC and refluxing with a $CaCl_2$ tube at 80 °C for 3 h. After the reaction, excess thionyl chloride was evaporated with a rotary evaporator. The reaction yielded 38 mg of the acyl chlorinated carbon flakes (OCC-Cl).

Synthesis of Ionic Liquid AmimCl. Synthesis of ionic liquid (IL) AmimCl followed a previously published synthesis route.[9] A typical procedure was as follows: 1-methylimidazole (32 mL, 0.4 mol, 1.0 equiv) was added in a round-bottom flask equipped with a magnetic stirrer. Allyl chloride (41 mL, 0.5 mol, 1.25 equiv) was added slowly under stirring at RT. The reaction was heated to 55 °C for 18−24 h with a reflux condenser and a $CaCl_2$ tube. Excess allyl chloride was evaporated with a rotary evaporator. If unreacted 1-methylimidazole remained, it was removed by extracting with 3 × 50 mL of ethyl acetate. The AmimCl was dried in vacuum oven and stored in a desiccator.

Synthesis of OCC-Modified (CA-OCC) and Neat Cellulose Acetate (CA). α-Cellulose and paper towels were dried in vacuum oven at room temperature (RT) for minimum of 8 h. The dissolution of cellulose in ionic liquid was done under vacuum at 80−100 °C overnight until the solution became clear. Synthesis of OCC-modified CA with covalently attached OCC followed a previously published procedure for cellulose esterification.[2,3] In short, a 3.5−4.5 wt % solution of cellulose in AmimCl was prepared. Water was removed from the reaction during the dissolution of the solution at 80−100 °C under vacuum overnight, after which the atmosphere was changed to N_2. For certain samples (Figure 2b), further drying was done by purging the solution with N_2 for 20 min prior to starting the reaction. The reaction was started by adding pyridine (1.5 equiv) and acetic anhydride (5 equiv) in the reaction mixture through a septum, and the reaction was left to proceed for 2 h at 80 °C. For the synthesis of the reference products (neat CAs), the reaction was stopped here. For the OCC-modified CA composite synthesis, OCC was added to the reaction flask, and the reaction was continued for an additional 2.5 h. The product was purified by precipitation in MeOH, filtration, washing with MeOH, dissolution in DMSO, reprecipitation in MeOH, filtration, and washing again with MeOH. The products were dried in vacuum at RT for 48 h before characterization.

The products were named according to their backbone (cellulose or cellulose acetate (CA)), their DS for acetate groups (high (H; DS ≥ 1.9), low (L, DS < 1.5) and the amount of OCC used in the synthesis (wt %), for example, CAH−OCC2. Additionally, the two products synthesized using paper towels as cellulose source, are marked with PT in their name, for example, CAH(PT)-OCC2.

Measurements and Characterization. ^{1}H and ^{13}C NMR spectra were recorded on Bruker Advance 400 MHz spectrometer with 16 scans in DMSO-d_6 at RT. For cellulose samples, a couple of drops of trifluoroacetic acid (TFA) were added to shift the peak of exchangeable protons downfield in ^{1}H NMR. The degree of substitution (DS) for acetylation of CAs was calculated from the ^{1}H NMR spectra. ^{13}C NMR at 90 °C was recorded on Bruker 500 MHz Avance III.

The Fourier-transform infrared spectra (FTIR) were collected with PerkinElmer Spectrum 2000 FTIR spectrometer, with attenuated total reflectance (ATR) accessory from Graseby Specac. A total of 16 scans were recorded in the wavenumber area of 600 to 4000 cm^{-1}.

Thermogravimetric analysis (TGA) was performed with Mettler-Toledo TGA/SDTA 851w instrument. The sample size was 2−5 mg and the measurements were done in N_2 atmosphere with a flow rate of 50 mL/min. The samples were heated from 30 to 600 °C at a rate of 10 °C/min.

Differential scanning calorimetry (DSC) was performed with Mettler Toledo DSC instrument. The sample size was 1−5 mg, and the analyses were performed in a N_2 atmosphere with a flow rate of 50 mL/min. The method was as follows: the sample was kept at 30 °C for 2 min, then heated up to 300 °C with a rate of 20 °C/min, kept at 300 °C for 2 min, and then the temperature was decreased to 30 °C with a rate of 20 °C/min, kept at 30 °C for 2 min, and then heated up again to 300 °C with the rate of 20 °C/min.

X-ray diffraction (XRD) spectra were acquired on a PANalytical X'Pert Pro diffractometer at RT using a silicum monocrystal sample holder. CuKR (λ = 0.1541 nm) was used as an X-ray source. The intensities were measured in a 2θ angular range with a step size of 0.017°.

Scanning electron microscopy (SEM) images were acquired by an ultrahigh resolution FE-SEM Hitachi S-4800. The samples were sputter-coated with a 5 nm Pt/Pd layer prior analysis.

Confocal Raman spectroscopy analyses were acquired on a HR800 UV Jobin Yvon Raman (Horiba, Kyoto, Japan) combined with a solid-state laser (514) nm. A 50× objective and a 600 groove mm^{-1} density grating was used for all measurements. The spectra were G-band intensity normalized.

X-ray photoelectron spectroscopy (XPS) were measured using AXIS Ultra equipped with DLD (Kratos Analytical, Manchester, U.K.). The measurements were recorded using low-power monochromatic Al Kα irradiation at 100 W and under neutralization. The survey spectra were recorded with a step size of 1 eV and an analyzer pass energy of 80 eV, whereas the high-resolution regions of C 1s and O 1s were recorded with a 0.2 eV step and 20 eV pass energy. The binding energy scale was referenced to C 1s at 286.7 eV (C−O). Data analysis was performed with CasaXPS software.

Film Preparations. Films were prepared by modifying a previously reported procedure of casting films using IL.[43] In short, 0.5 g of sample was dissolved in 4.5 g 30% DMSO in AmimCl at 80−100 °C overnight. The films were cast on a Petri dish (⌀ = 4 cm). The solution was cooled down with dry ice and put into a regeneration water bath at 40 °C for 1 h. After that, the water was changed, and the film was washed for 3 h at 60 °C. The water was then changed again, and washing was continued for 24 h at RT. Finally, the films were dried at 60 °C.

Tensile Testing. The mechanical properties of CAL-OCC2 were evaluated by tensile testing. Specimens (thickness 80−100 mm; width 5 mm) were of rectangular shape and measured on an Instron universal test instrument (model 5944, Instron Instruments) with a load cell of 500 N, a crosshead speed of 5 mm/min, and a gauge length of 10 mm. The specimens were preconditioned at 23 °C and a relative humidity of 50% for 3 days prior to testing. A total of six measurements were conducted.

RESULTS AND DISCUSSION

Thermoplastic cellulose acetate (CA) composites with covalently attached oxidized carbonized cellulose (OCC) were synthesized in the ionic liquid (IL) 1-allyl-3-methylimidazolium chloride (AmimCl). The composites were synthesized in a one-batch continuous process and processed into films for thermal and mechanical characterization.

Synthesis of the Acyl Chlorinated OCC (OCC-Cl). The cellulose-derived OCC were first synthesized by microwave-

https://dx.doi.org/10.1021/acs.biomac.9b01672
Biomacromolecules 2020, 21, 1752−1761

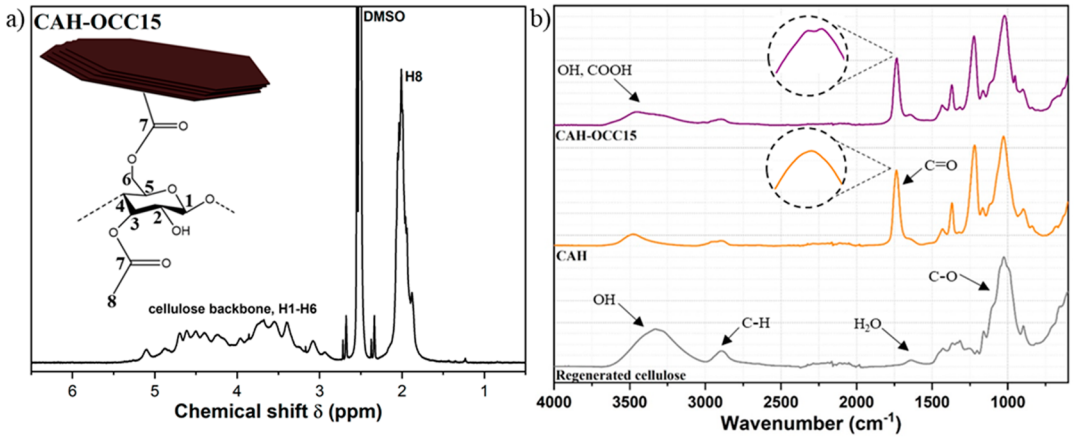

Figure 3. (a) ^{1}H NMR of CAH-OCC15. (b) FTIR spectra of the OCC-modified CA composite, CAH-OCC15, the neat CA reference product, CAH, and regenerated cellulose.

assisted hydrothermal carbonization (HTC; Figure 1a).[25,26,36,44] During HTC, crystalline cellulose was transformed into carbonized powder of carbon spheres[36] and flake-like structures with greatly altered properties and appearance compared to the original cellulose. The carbonized products were then oxidized, and the OCC was purified by dialysis in water. The OCC was in an amorphous state, as confirmed by the absence of crystalline peaks in the WAXD spectrum (Figure S5). Based on the SEM images, the OCC was mainly microsized and polydisperse in shape and size (Figure 1c,d), displaying a size range from below one micrometer to tens of micrometers.

Before reaction with CA, the OCC were successfully surface functionalized to acyl chlorinated OCC (OCC-Cl) to increase the reactivity toward the OH groups of CA (Figure 1a). The reaction with thionyl chloride was shown to be fast and convenient due to the volatile byproducts SO_2 and HCl, which made the purification by rotary evaporator easy. According to the FTIR spectrum (Figure 1b), the OCC particles contained carboxyl (broad O−H stretch at 3300−2400 cm^{-1}, C═O stretch at 1710 cm^{-1}), hydroxyl (broad O−H stretch at around 3300 cm^{-1}, C−O stretch, and O−H bending around 1100 cm^{-1}), aromatic (C═C stretch at 1630 cm^{-1}), aliphatic groups (C−H stretch at 2970 cm^{-1}), and epoxy (C−O stretch at 1106 cm^{-1}).[36,37] Raman analysis further supported the content of sp^2 structures in both of the OCC particles with G and D bands at 1593 and 1367 cm^{-1}, respectively (Figure S6). The G band corresponds to the in-plane bond stretching motion of C═C in rings and chains, and the D band is related to the breathing modes of C═C in rings.[45]

As a confirmation of the successful reaction, the appearance of the acyl chloride peak for OCC-Cl in the FTIR in the carbonyl area (1780 cm^{-1}) was clearly visible, and the broad OH-stretching peak decreased in size. Furthermore, XPS analysis of OCC and OCC-Cl particles further confirmed the successful reaction as the XPS spectrum of OCC-Cl showed chlorine (Cl 2p) at the binding energy 200 eV, whereas this peak was absent for OCC (Figure S13). Typically, the content of inorganic chlorine is present below 200 eV,[46,47] which supports covalent attachment of chlorine on the OCC particles. The rest of the functional groups in OCC and OCC-Cl that were encountered in FTIR spectra were also confirmed by XPS analysis (Table S2). Furthermore, both S 2p (167−168 eV) and N 1s (406 and 401 eV) were present in OCC and OCC-Cl, most likely originating from the H_2SO_4 and HNO_3 used during preparation. The morphology of the carbonized particles did not exhibit obvious changes during the acyl chlorination reaction, as shown by SEM images (Figure 1c,d).

Synthesis of OCC-Modified CA Composites. A series of covalently modified CA with different amounts of OCC were successfully synthesized in the IL AmimCl (Figure 2). Earlier studies have also shown that AmimCl facilitates cellulose functionalization giving excellent yields, low viscosity reaction medium, easy product recovery and generally mild reaction conditions.[2,6,9] The main benefit of using ILs over other solvents is that they are nonderivatizing[9] and they can potentially be recovered.[48,49] In total, 6 OCC-modified CAs with different DS for acetylation (0−2.4) and different amounts of OCC (1−18 wt % in feed) were synthesized and characterized. As references, 3 neat CA (without OCC) with DS ranging from 1.1 to 2.0 were synthesized. Additionally, a physical composite was manufactured by mixing CAL and 2 wt % OCC (CAL + 2wt% OCC) (Figure 2).

For obtaining homogeneous reaction conditions, the efficiency of the dissolution of cellulose in AmimCl is a key factor and was therefore studied. The dissolution of cellulose in AmimCl was shown to be efficient and reached up to 4.5 wt %. From the SEM analysis, it could be concluded that the cellulose fibrous structure was disrupted after dissolution in AmimCl and a continuous matrix of regenerated cellulose was formed (Figure S3). Furthermore, the WAXD analysis displayed no remaining crystalline peaks of cellulose (Figure S10).

AmimCl has previously been shown to dissolve up to 14.5 wt % of cellulose, but the amount depends on the crystallinity and DP of cellulose, as well as water content.[3,9] The cellulose material used in the current study had a crystallinity as high as 64%, as determined by a relative WAXD method,[36] which may have influenced the dissolution capacity. The hygroscopicity and sensitivity of ILs toward impurities are also challenging when using ILs as a reaction medium.[3,5,50] To avoid these issues, the IL was freshly synthesized or as an alternative swept with nitrogen gas for 30−45 min prior to starting the reaction, which has been shown to efficiently dry solvents.[50] Other successful drying methods have also been suggested, such as freeze-drying.[3]

https://dx.doi.org/10.1021/acs.biomac.9b01672
Biomacromolecules 2020, 21, 1752−1761

A base-catalyzed one-pot esterification of cellulose was performed utilizing acetic anhydride and OCC-Cl as the esterification agents. First, the acetylation reaction was let to proceed for 2 h, then OCC-Cl was added in the same flask to react with remaining hydroxyl groups in CA for further 2.5 h. ^{1}H and ^{13}C NMR confirmed the successful acetylation reaction through the presence of the acetyl groups[2,51] in both OCC-modified CA composites and in neat CA (Figures 3a and S7–S9). No significant broadening or multiple ester peaks were witnessed in the NMR spectra of OCC-modified CA compared with neat CA, probably due to the small amount and polydispersity of OCC particles. It was shown that all the synthesized products with DS > 1.0 were soluble in DMSO after drying, and nonsoluble in water, acetic acid, chloroform, and acetone.

Further confirmation of successful esterification was provided by FTIR spectroscopy (Figure 3b): a peak in the carbonyl area was detected both for CA and OCC-modified CA composites and showed the presence of an ester bond. In the case of CA, this peak was located at 1736 cm^{-1}. With further investigation of this peak in OCC-modified composites, a doublet nature could be revealed with the peaks at 1738 and 1733 cm^{-1}, which indicates two types of esters bound on the polymer backbone originating from acetylation and attachment of OCC. In FTIR, the OH-stretch band at around 3500 cm^{-1} differs substantially in shape for OCC-modified CA composites and neat CA, which further indicates the presence of OCC that typically exhibits a large and broad peak in this area.

The OCC-modified CA composites and neat CA were clearly distinguished by the color difference (Figure 2c). The OCC-modified product CAL-OCC2 was remarkably darker in color compared with neat CAL sample. Additionally, no tendency of OCC migration from the OCC-modified CA matrix was noticed during dissolution of OCC-modified CA in tested solvents (DMSO, water, acetone, chloroform, acetic acid), indicating a successful covalent linkage with OCC. However, exact quantification of the amount of OCC attached could not be done, and the weight percentages therefore refer to the amount of OCC used in the reaction. A reverse reaction order was also evaluated, but it resulted in low DS of acetylation (0.8) probably due to acetylation of the OCC-Cl flakes.

It was further confirmed that there were no significant amounts of acetic anhydride left to react further upon addition of OCC-Cl. According to NMR analysis of the reaction mixture after the cellulose acetylation reaction, the acetic anhydride was nearly completely consumed during the 2 h of acetylation. A trace signal corresponding to acetic anhydride could be seen, but integration shows less than 1 mol % of acetic anhydride in the reaction mixture as compared to AmimCl (Figure S12). Furthermore, due to the high reactivity of OCC-Cl, any potentially remaining acyl chloride groups are expected to react with MeOH or water during the precipitation and washing.

Thermal Properties. The OCC-modified CA composites and neat CA products with DS ≥ 1.4 displayed clear glass transition temperatures (T_g), as typically observed for thermoplastic products (Figures 2b and 4a). The thermoplastic properties are generally enhanced as the acetyl content increases due to breakage of hydrogen bonding and increased free volume caused by the acetyl groups.[2,11] Pure cellulose does not display any clear phase transitions, as it degrades before these occur.[2]

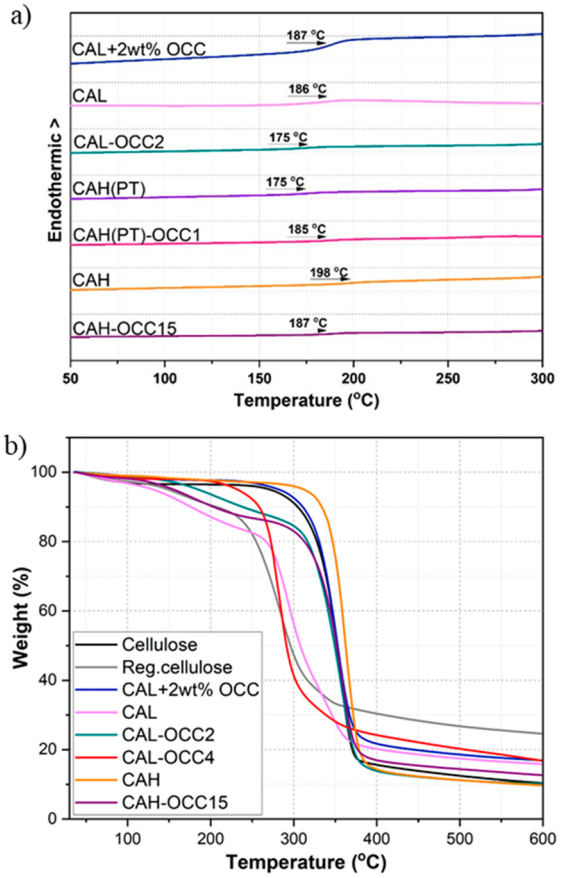

Figure 4. (a) DSC thermograms of different OCC-modified and neat CA materials, as well as a physical blend of CAL/OCC (CAL + 2 wt % OCC). (b) TGA curves of selected products in N_2 atmosphere.

It has been previously suggested that graphite/graphene oxide (GO) sheets might restrict the associate formation of CA and lead to higher mobility of the chains, thus causing a decrease in T_g.[20] The OCC might act in the same manner and a decreased T_g was, in fact, observed in some cases, but the effect was not as prominent as in the case of GO-modified CA. This is most likely because the T_g of the OCC-modified CA composite is a function of not only the amount of OCC, but also the DP and DS of the polymer. For example, CAL and CAL-OCC2 had similar DS, but the OCC-modified CA composite showed 6 °C lower T_g compared to the neat CA (CAL). Furthermore, a physical mixture of CAL and 2 wt % OCC was used as a reference. The product with covalently attached OCC had 12 °C lower T_g than the physical mixture, suggesting better thermoplastic properties for the composites with covalently attached OCC.

For CAH-OCC15, the synergistic contribution of 15 wt % OCC in feed, together with the higher DS, led to a 12 °C decrease in T_g as compared to the reference product CAH. More unexpected results were, however, witnessed in the case of the paper tissue derived products, as CAH(PT)-OCC1 showed 10 °C higher T_g than the reference sample CAH(PT) of lower DS for acetylation. It could be speculated that for cellulose products with lower DP, as is the case of the processed cellulose from PT, the OCCs could hinder the mobility of the polymer chain. T_g was not observed for CAL-OCC4 probably because of the low DS of 1.1. Additionally, when comparing the reference products CAH and CAH(PT),

https://dx.doi.org/10.1021/acs.biomac.9b01672
Biomacromolecules 2020, 21, 1752–1761

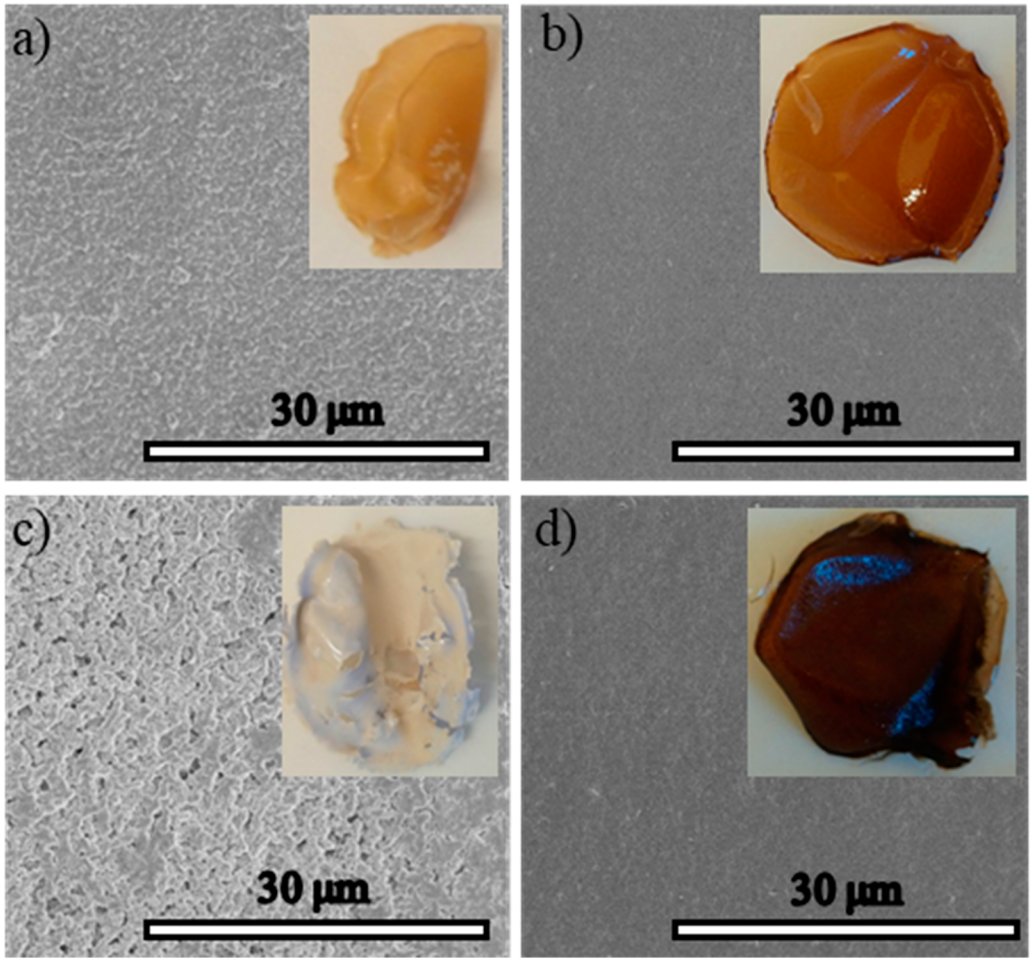

Figure 5. SEM images of the surfaces of the films: (a) CAL, (b) CAL-OCC2, (c) CAL + 2 wt % OCC (noncovalent mixture), and (d) CAL-OCC4.

there was a 23 °C difference in the T_g values, even though the DS for acetylation was similar. The lower T_g for CAH(PT) can be explained by its lower DP and, thus, in many cases, the differences in T_g caused by OCC-modification could be hidden behind the more prominent effects from, for example, DP and DS.

The thermal stability of the OCC-modified CA composites and neat CA was further investigated by thermogravimetry (Figures 4b and S11). All the OCC-modified CA composites and CAL showed a first degradation step in the TGA curves at approximately 130−140 °C, apart from CAL-OCC4 and the physical mixture, CAL + 2 wt % OCC. The first degradation step is probably due to the presence of labile oxygen-containing functional groups on both CA and OCC that are lost at temperature range of 100−200 °C.[27] A decreasing thermal stability trend was observed when incorporating OCC in the highly acetylated cellulose chains (e.g., CAH−OCC15). CAs of higher DS have excellent thermal stability, even compared to native cellulose, while the incorporation of OCC increases the amount of thermally labile oxygen-functionalities.

The OCC-modified CA composites with low degree of acetylation (CAL) showed diverged thermal stability compared to neat CAL. The final decomposition (second degradation step) on-set temperatures were 250, 290, and 250 °C for CAL, CAL-OCC2, and CAL-OCC4, respectively. The higher stability of CAL-OCC2 and the absence of the first degradation step for CAL-OCC4 might be due to the interfacial interactions between the polar functional groups of CAL backbone and OCC, as has been suggested before for GO-cellulose composites.[28,30] However, the thermal behavior and the low DS of acetylation of CAL-OCC4 might also indicate that the sample has a smaller amount of OCC particles attached on the CA backbone than CAL-OCC2, leading to its distinctive thermal stability. The covalently linked OCC are assumed to be homogeneously distributed on the polymer backbone forming thermally insulating layers of OCC, which could increase the thermostability.[27] The literature shows that the addition of graphene derivatives generally increases the thermal stability of cellulose composites.[24,28,31]

Regenerated cellulose showed a significant decrease in thermal stability (218 °C) compared to native cellulose (250 °C), probably because of the disruption of the fibrous structure and strong hydrogen bonding that makes cellulose thermostable. Both the high and the low DS CA (CAH and CAL, respectively) displayed better thermal stabilities compared to the regenerated cellulose, because the thermally unstable hydroxyl groups had been acetylated. CAH showed even higher thermal stability (290 °C) than the native cellulose (250 °C), which is in accordance with previous publications.[11] Interestingly, the physical mixture, CAL + 2 wt % OCC, also showed higher thermal stability (285 °C) than native cellulose, probably due to the favorable interfacial interactions previously discussed.

https://dx.doi.org/10.1021/acs.biomac.9b01672
Biomacromolecules 2020, 21, 1752−1761

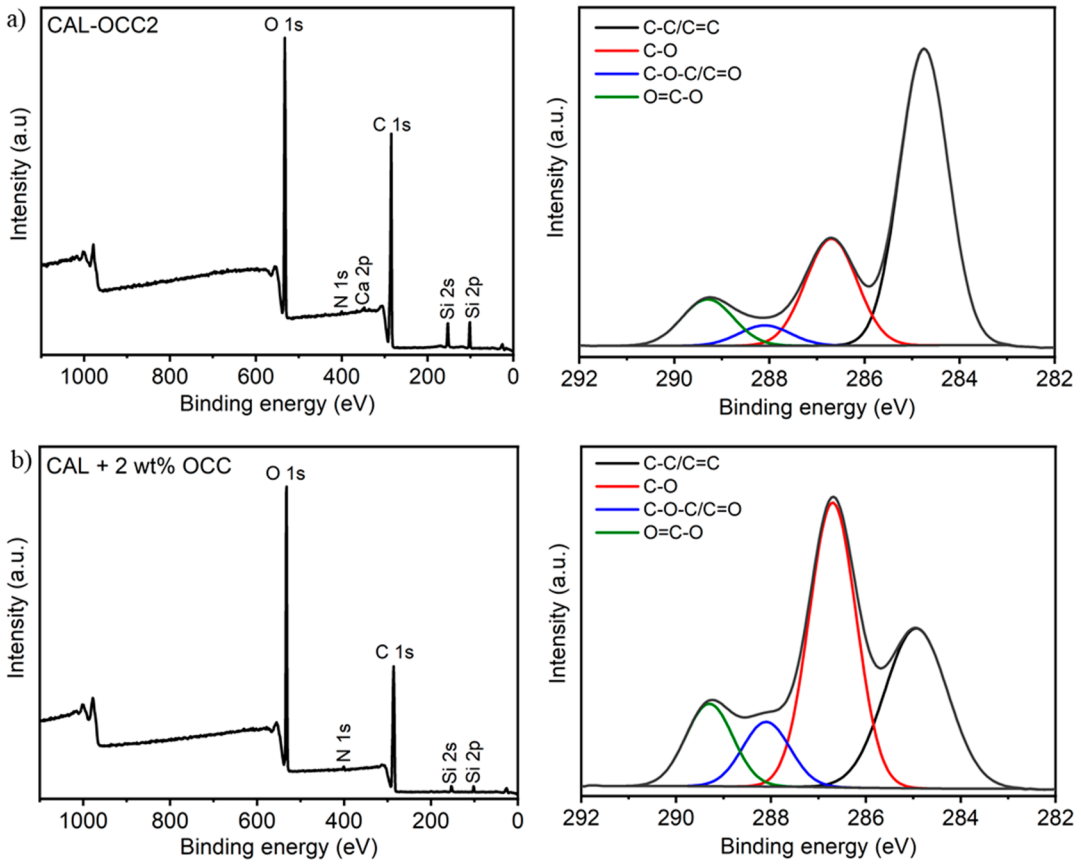

Figure 6. XPS survey spectra (left) and narrow scans C 1s (right) of CAL-OCC2 (a) and CAL + 2 wt % OCC (b).

The residual chars of the composites were between that of native cellulose and regenerated cellulose, but no clear trends could be deduced from the data (Figure 4b). The increase in the amount of residual char was commonly observed for composites loaded with graphite derivatives.[30,31,52] It has also been suggested that the interactions between the cellulose backbone and GO particles might induce additional carbonization and thus lead to higher char residues.[52] Thus, the additional carbonization could cause this divergence in the residual char amounts.

Physicochemical Properties of OCC-Modified CA Composites and Neat CA. Films of OCC-modified CA composites were prepared to evaluate their mechanical performance. The two OCC-modified CA composite films, CAL-OCC2 and CAL-OCC4, as well as reference films of neat CA, CAL, and a physical blend of CAL and 2 wt % OCC were solution-casted using an IL/DMSO mixture. To establish the effect of covalently attached OCC versus physically blended OCC, a noncovalent, CAL + 2 wt % OCC composite was prepared.

Clear differences in the appearances and structures of the films were seen (Figure 5). It was noteworthy that the covalent OCC-modification led to clearly enhanced film quality with transparent films in the case of CAL-OCC2 and CAL-OCC4. This is unusual for CA films with a low degree of acetylation. Typically, DS > 2.0 is needed to yield good quality films.[10] The transparency indicated a uniform dispersion of OCC in the matrix, good compatibility, and favorable interactions between CA and OCC.[20] The neat CAL film was yellowish, thick, and shrank during the drying, whereas the physical blend composite, CAL + 2 wt % OCC, was white, thin, and fractured, but retained its shape during drying. According to the SEM images, the OCC-modified covalent composite films CAL-OCC2 and CAL-OCC4 showed a smooth and homogeneous surface, whereas the reference films, CAL and CAL + 2 wt % OCC, were rough and uneven.

The preparation of the films gave further evidence of the successful covalent nature of the composites: during the manufacturing of the physical composite film, the unbound, water-soluble OCC leaked out during the washing of the CAL + 2 wt % OCC film. This was not noticed for the covalent composites CAL-OCC2 and CAL-OCC4. XPS analysis of CAL-OCC2 and CAL + 2 wt % OCC was therefore performed and it further indicated that covalent attachment was necessary for avoiding migration of OCC particles during film preparation (Figure 6 and Table S3). According to the analysis, both materials displayed C—C/C═C, C—O, C—O—C/C═O and O═C—O at the binding energies 284.8–284.9, 286.7, 288.1, and 289.3 eV. It could further be deduced that CAL-OCC2 films with covalently attached OCC displayed an O/C ratio of 0.34, and the physical mixture (CAL + 2 wt % OCC) had an O/C of 0.52. The higher O/C ratio for the physical mixture implied that the carbonized material OCC had a large part migrated from the material, which gave rise to the nontransparent and brittle film. The lower O/C ratio for CAL-OCC2 indicated covalent attachment of OCC, which provided good film-forming ability. Similarly, a cellulose-derived carbon nanofiber/GO composite has shown an increment of the C—C/C═C peak compared to neat cellulose due to the addition of carbon material.[53]

Mechanical properties of CAL-OCC2 were tested, as this material had very good film-forming ability and showed both

https://dx.doi.org/10.1021/acs.biomac.9b01672
Biomacromolecules 2020, 21, 1752–1761

a)

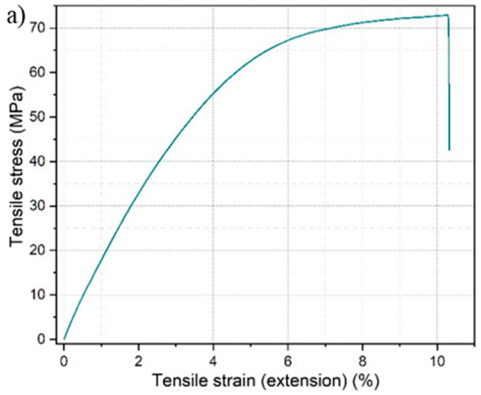

b)

Sample	Tensile strength (MPa)	Extension at break (%)	Young's modulus (GPa)
CAL-OCC2 (DS = 1.5)	71.4±7.0	11.0±3.1	1.53±0.15
Literature reference values			
CA DS=1.5	27	< 1.6	0.13
CA DS=2.2-2.5	21-55	2.4-5.0	0.3-0.95

Figure 7. (a) Closest-to-average curve from tensile testing of CAL-OCC2. (b) Numerical results of tensile test of CAL-OCC2, as well as literature reference values for neat CA films.[17,22,54,55]

transparency and flexibility. The other films were too brittle and uneven for cutting specimens and were therefore not tested for their mechanical performance. The higher brittleness of CAL-OCC4 might have been due to the lower degree of acetylation compared to CAL-OCC2. This is in good agreement with literature, as CA with DS 0.8 has been shown to be too brittle for mechanical tests.[17]

The closest-to-average stress−strain curve of CAL-OCC2 is presented in Figure 7a. The stress-at-break of the film was 71.4 ± 7.0 MPa, the elongation-at-break 11.0 ± 3.1% and Young's modulus 1.53 ± 0.15 GPa. The CAL-OCC2 showed thus clearly higher values in strength, stiffness and ductility as compared to literature values for pure cellulose acetate films with similar and higher DS (Figure 7b).[17,22,54,55] The mechanical performance of CAL-OCC2 was in line with the previously reported results on films of CA and cellulosic GO composites. Though, the properties of cellulose materials are dependent on many variables, such as DP, DS, crystallinity, manufacturing conditions as well as the size, shape and nature of the filler particles.[17,54,56] Generally, Young's modulus and tensile strength of cellulose derivatives increased with non-covalently added graphite derivatives,[28−31,52] while elongation-at-break decreased.[31,52,57] However, a study by Liu et al. showed that an optimized GO loading could increase the elongation-at-break compared to pure cellulose, leading to values up to 16%.[29]

Altogether, based on the quality of the CAL-OCC2 and CAL-OCC4 films, the covalent attachment of OCCs positively enhanced the film quality with respect to optical and mechanical properties. The visual transparency of the covalently OCC-modified composite films, CAL-OCC2 and CAL-OCC4, indicates good compatibility of OCC and CA backbone and uniform reaction during OCC-modification resulting in good dispersion of the OCC in the matrix.[22]

CONCLUSIONS

Thermoplastic "all-cellulose" composites were successfully synthesized through covalent modification of cellulose acetate (CA) by oxidized carbonized cellulose (OCC) prepared by HTC of cellulose and paper tissues. The OCC were of micrometer size, had plane morphology and oxygen functionalities that facilitated acyl chlorination and subsequent covalent attachment of acyl chlorinated OCC onto CA. The acetylation and OCC-modification of cellulose could be performed in a one-pot reaction in the IL AmimCl. It was shown that the covalent attachment of OCC to CA greatly improved the optical and mechanical properties of the composite films as compared to both neat CA and CA with physically blended OCC. The results indicate great future potential for the fabricated "all-cellulose" composite materials with thermoplastic properties. Furthermore, this could provide a potential upcycling possibility for paper waste products taking a step toward circular resource economy.

ASSOCIATED CONTENT

Supporting Information

The Supporting Information is available free of charge at https://pubs.acs.org/doi/10.1021/acs.biomac.9b01672.

NMR spectra of ionic liquid AmimCl, CA composites and references, IR spectra of cellulose before and after dissolution, SEM images of cellulose before and after dissolution, WAXD spectra of OCC and CA composites, TGA characterization for composites, tensile testing results for CAL-OCC2, analysis of remaining acetic anhydride after reaction, and XPS analysis of OCC, OCC-Cl, CAL-OCC2 and CAL + 2 wt % OCC (PDF)

AUTHOR INFORMATION

Corresponding Author

Minna Hakkarainen − *Department of Fibre and Polymer Technology, KTH Royal Institute of Technology 100 44 Stockholm, Sweden*; orcid.org/0000-0002-7790-8987; Email: minna@kth.se

Authors

Lotta H. Gustavsson − *Department of Fibre and Polymer Technology, KTH Royal Institute of Technology 100 44 Stockholm, Sweden*

Karin H. Adolfsson − *Department of Fibre and Polymer Technology, KTH Royal Institute of Technology 100 44 Stockholm, Sweden*

Complete contact information is available at: https://pubs.acs.org/10.1021/acs.biomac.9b01672

Author Contributions

The manuscript was written through contributions of all authors. All authors have given approval to the final version of the manuscript.

Notes

The authors declare no competing financial interest.

https://dx.doi.org/10.1021/acs.biomac.9b01672
Biomacromolecules 2020, 21, 1752−1761

■ ACKNOWLEDGMENTS

The authors thank Sergey Dvinskikh & Istvan Furo for assistance in NMR measurements. Leena-Sisko Johansson and Joseph M. Campbell are thanked for XPS measurements and analysis.

■ ABBREVIATIONS

AmimCl, 1-allyl-2-methylimidazolium chloride; CA, cellulose acetate; OCC, oxidized carbonized cellulose; GO, graphene/graphite oxide; IL, ionic liquid; DS, degree of substitution; PLA, polylactide

■ REFERENCES

(1) Klemm, D.; Heublein, B.; Fink, H.-P.; Bohn, A. Cellulose: Fascinating Biopolymer and Sustainable Raw Material. *Angew. Chem., Int. Ed.* **2005**, *44*, 3358−3393.
(2) Chen, Z.; Zhang, J.; Xiao, P.; Tian, W.; Zhang, J. Novel Thermoplastic Cellulose Esters Containing Bulky Moieties and Soft Segments. *ACS Sustainable Chem. Eng.* **2018**, *6*, 4931−4939.
(3) Barthel, S.; Heinze, T. Acylation and Carbanilation of Cellulose in Ionic Liquids. *Green Chem.* **2006**, *8*, 301−306.
(4) Xu, A.; Chen, L.; Wang, J. Functionalized Imidazolium Carboxylates for Enhancing Practical Applicability in Cellulose Processing. *Macromolecules* **2018**, *51* (11), 4158−4166.
(5) Swatloski, R. P.; Spear, S. K.; Holbrey, J. D.; Rogers, R. D. Dissolution of Cellulose with Ionic Liquids. *J. Am. Chem. Soc.* **2002**, *124* (18), 4974−4975.
(6) Wu, J.; Zhang, J.; Zhang, H.; He, J.; Ren, Q.; Guo, M. Homogeneous Acetylation of Cellulose in a New Ionic Liquid. *Biomacromolecules* **2004**, *5* (2), 266−268.
(7) Yousefi, H.; Nishino, T.; Faezipour, M.; Ebrahimi, G.; Shakeri, A. Direct Fabrication of all-Cellulose Nanocomposite from Cellulose Microfibers Using Ionic Liquid-Based Nanowelding. *Biomacromolecules* **2011**, *12* (11), 4080−4085.
(8) Niu, X.; Liu, Y.; King, A. W. T.; Hietala, S.; Pan, H.; Rojas, O. J. Plasticized Cellulosic Films by Partial Esterification and Welding in Low-Concentration Ionic Liquid Electrolyte. *Biomacromolecules* **2019**, *20* (5), 2105−2114.
(9) Zhang, H.; Wu, J.; Zhang, J.; He, J. 1-Allyl-3-methylimidazolium Chloride Room Temperature Ionic Liquid: A New and Powerful Nonderivatizing Solvent for Cellulose. *Macromolecules* **2005**, *38* (20), 8272−8277.
(10) Fischer, S.; Thümmler, K.; Volkert, B.; Hettrich, K.; Schmidt, I.; Fischer, K. Properties and Applications of Cellulose Acetate. *Macromol. Symp.* **2008**, *262*, 89−96.
(11) Kamide, K.; Saito, M. Thermal Analysis of Cellulose Acetate Solids with Total Degrees of Substitution of 0.49, 1.75, 2.46 and 2.92. *Polym. J.* **1985**, *17* (8), 919−928.
(12) Gu, J.-D.; Eberiel, D. T.; McCarthy, S. P.; Gross, R. A. Cellulose Acetate Biodegradability upon Exposure to Simulated Aerobic Composting and Anaerobic Bioreactor Environments. *J. Environ. Polym. Degr.* **1993**, *1* (2), 143−153.
(13) Puls, J.; Wilson, S. A.; Hölter, D. Degradation of Cellulose Acetate-Based Materials: A Review. *J. Polym. Environ.* **2011**, *19*, 152−165.
(14) Fei, Z.; Huang, S.; Yin, J.; Xu, F.; Zhang, Y. Preparation and Characterization of Bio-based Degradable Plastic Films Composed of Cellulose Acetate and Starch Acetate. *J. Polym. Environ.* **2015**, *23*, 383−391.
(15) de Freitas, R. R. M.; Senna, A. M.; Botaro, V. R. Influence of Degree of Substitution on Thermal Dynamic Mechanical and Physicochemical Properties of Cellulose Acetate. *Ind. Crops Prod.* **2017**, *109*, 452−458.
(16) Ifuku, S.; Nogi, M.; Abe, K.; Handa, K.; Nakatsubo, F.; Yano, H. Surface Modification of Bacterial Cellulose Nanofibers for Property Enhancement of Optically Transparent Composites: Dependence on Acetyl-Group DS. *Biomacromolecules* **2007**, *8* (6), 1973−1978.
(17) Morgado, D.; Rodrigues, B.; Almeida, E.; Seoud, O.; Frollini, E. Bio-based Films from Linter Cellulose and Its Acetates: Formation and Properties. *Materials* **2013**, *6*, 2410−2435.
(18) Chen, S.; Schueneman, G.; Pipes, R. B.; Youngblood, J.; Moon, R. J. Effects of Crystal Orientation on Cellulose Nanocrystals-Cellulose Acetate Nanocomposite Fibers Prepared by Dry Spinning. *Biomacromolecules* **2014**, *15* (10), 3827−3835.
(19) Liu, L.; Shen, Z.; Liang, S.; Yi, M.; Zhang, X.; Ma, S. Enhanced Atomic Oxygen Erosion Resistance and Mechanical Properties of Graphene/Cellulose Acetate Composite Films. *J. Appl. Polym. Sci.* **2014**, *131*, 40292.
(20) de Moraes, A. C. M.; Andrade, P. F.; de Faria, A. F.; Simões, M. B.; Salomão, F. C. C.; Barros, E. B.; Gonçalves, M. d. C.; Alves, O. L. Fabrication of Transparent and Ultraviolet Shielding Composite Films Based on Graphene Oxide and Cellulose Acetate. *Carbohydr. Polym.* **2015**, *123*, 217−227.
(21) Liu, L.; Shen, Z.; Liang, S.; Yi, M.; Zhang, X.; Ma, S. Graphene for Reducing Bubble Defects and Enhancing Mechanical Properties of Graphene/Cellulose Acetate Composite Films. *J. Mater. Sci.* **2014**, *49*, 321−328.
(22) Hassan, M.; Berglund, L.; Abou-Zeid, R.; Hassan, E.; Abou-Elseoud, W.; Oksman, K. Nanocomposite Film Based on Cellulose Acetate and Lignin-Rich Rice Straw Nanofibers. *Materials* **2019**, *12*, 595.
(23) Park, H.-M.; Misra, M.; Drzal, L. T.; Mohanty, A. K. Green" Nanocomposites from Cellulose Acetate Bioplastic and Clay: Effect of Eco-Friendly Triethyl Citrate Plasticizer. *Biomacromolecules* **2004**, *5* (6), 2281−2288.
(24) Pang, J.; Wang, X.; Li, L.; Wu, M.; Jiang, J.; Ji, Z.; Yu, S.; Yu, H.; Zhang, X. Tough and Conductive Bio-based Artificial Nacre via Synergistic Effect Between Water-Soluble Cellulose Acetate and Graphene. *Carbohydr. Polym.* **2019**, *206*, 319−327.
(25) Xu, H.; Adolfsson, K. H.; Xie, L.; Hassanzadeh, S.; Pettersson, T.; Hakkarainen, M. Zero-Dimensional and Highly Oxygenated Graphene Oxide for Multifunctional Poly(lactic acid) Bionanocomposites. *ACS Sustainable Chem. Eng.* **2016**, *4* (10), 5618−5631.
(26) Hassanzadeh, S.; Adolfsson, K. H.; Wu, D.; Hakkarainen, M. Supramolecular Assembly of Biobased Graphene Oxide Quantum Dots Controls the Morphology of and Induces Mineralization on Poly(ε-caprolactone) Films. *Biomacromolecules* **2016**, *17* (1), 256−261.
(27) Wu, D.; Bäckström, E.; Hakkarainen, M. Starch Derived Nanosized Graphene Oxide Functionalized Bioactive Porous Starch Scaffolds. *Macromol. Biosci.* **2017**, *17*, 1600397.
(28) Han, D.; Yan, L.; Chen, W.; Li, W.; Bangal, P. R. Cellulose/Graphite Oxide Composite Films with Improved Mechanical Properties over a Wide Range of Temperature. *Carbohydr. Polym.* **2011**, *83* (2), 966−972.
(29) Liu, X.; Zhang, T.; Pang, K.; Duan, Y.; Zhang, J. Graphene Oxide/Cellulose Composite Films with Enhanced UV-Shielding and Mechanical Properties Prepared in NaOH/Urea Aqueous Solutions. *RSC Adv.* **2016**, *6*, 73358−73364.
(30) Layek, R. K.; Ramakrishnan, K. R.; Sarlin, E.; Orell, O.; Kanerva, M.; Vuorinen, J.; Honkanen, M. Layered Structure Graphene Oxide/Methylcellulose Composites with Enhanced Mechanical and Gas Barrier Properties. *J. Mater. Chem. A* **2018**, *6*, 13203.
(31) Phiri, J.; Johansson, L.-S.; Gane, P.; Maloney, T. A Comparative Study of Mechanical, Thermal and Electrical Properties of Graphene-, Graphene Oxide- and Reduced Graphene Oxide-Doped Microfibrillated Cellulose Nanocomposites. *Composites, Part B* **2018**, *147*, 104−113.
(32) Xu, H.; Feng, Z.-X.; Xie, L.; Hakkarainen, M. Graphene-Oxide-Driven Design of Strong and Flexible Biopolymer Barrier Films: From Smart Crystallization Control to Affordable Engineering. *ACS Sustainable Chem. Eng.* **2016**, *4* (1), 334−349.
(33) Park, H.-M.; Liang, X.; Mohanty, A. K.; Misra, M.; Drzal, L. T. Effect of Compatibilizer on Nanostructure of the Biodegradable

https://dx.doi.org/10.1021/acs.biomac.9b01672
Biomacromolecules 2020, 21, 1752−1761

Cellulose Acetate/Organoclay Nanocomposites. *Macromolecules* **2004**, *37* (24), 9076−9082.
(34) Farooq, M.; Zou, T.; Riviere, G.; Sipponen, M. H.; Österberg, M. Strong, Ductile and Waterproof Cellulose Nanofibril Composite Films with Colloidal Lignin Particles. *Biomacromolecules* **2019**, *20* (2), 693−704.
(35) Huang, H.-D.; Liu, C.-Y.; Li, D.; Chen, Y.-H.; Zhong, G.-J.; Li, Z.-M. Ultra-low Gas Permeability and Efficient Reinforcement of Cellulose Nanocomposite Films by Well-aligned Graphene Oxide Nanosheets. *J. Mater. Chem. A* **2014**, *2*, 15853−15863.
(36) Adolfsson, K. H.; Hassanzadeh, S.; Hakkarainen, M. Valorization of Cellulose and Waste Paper to Graphene Oxide Quantum Dots. *RSC Adv.* **2015**, *5*, 26550−26558.
(37) Sevilla, M.; Fuertes, A. B. The production of carbon materials by hydrothermal carbonization of cellulose. *Carbon* **2009**, *47* (9), 2281−2289.
(38) Wu, D.; Samanta, A.; Srivastava, R. K.; Hakkarainen, M. Nano-Graphene Oxide Functionalized Bioactive Poly(lactic acid) and Poly(ε-caprolactone) Nanofibrous Scaffolds. *Materials* **2018**, *11* (4), 566.
(39) Erdal, N. B.; Hakkarainen, M. Construction of Bioactive and Reinforced Bioresorbable Nanocomposites by Reduced Nano-Graphene Oxide Carbon Dots. *Biomacromolecules* **2018**, *19* (3), 1074−1081.
(40) Feng, Z.; Hakkarainen, M.; Grützmacher, H.; Chiappone, A.; Sangermano, M. Photocrosslinked Chitosan Hydrogels Reinforced with Chitosan-Derived Nano-Graphene Oxide. *Macromol. Chem. Phys.* **2019**, *220*, 1900174.
(41) Larsson, P. A.; Berglund, L. A.; Wågberg, L. Ductile All-Cellulose Nanocomposite Films Fabricated from Core-Shell Structured Cellulose Nanofibrils. *Biomacromolecules* **2014**, *15* (6), 2218−2223.
(42) Granström, M.; Kavakka, J.; King, A.; Majoinen, J.; Mäkelä, V.; Helaja, J.; Hietala, S.; Virtanen, T.; Maunu, S.-L.; Argyropoulos, D. S.; Kilpeläinen, I. Tosylation and Acylation of Cellulose in 1-Allyl-3-methylimidazolium Chloride. *Cellulose* **2008**, *15* (3), 481−488.
(43) Wawro, D.; Hummel, M.; Michud, A.; Sixta, H. Strong Cellulosic Film Cast from Ionic Liquid Solutions. *Fibres Text. East. Eur.* **2014**, *22* (3), 35−46.
(44) Erdal, N. B.; Adolfsson, K. H.; Pettersson, T.; Hakkarainen, M. Green Strategy to Reduced Nanographene Oxide through Microwave Assisted Transformation of Cellulose. *ACS Sustainable Chem. Eng.* **2018**, *6*, 1246−1255.
(45) Ferrari, A. C. Raman spectroscopy of graphene and graphite: Disorder, electron-phonon coupling, doping and nonadiabatic effects. *Solid State Commun.* **2007**, *143*, 47−57.
(46) Araujo, J. R.; Archanjo, B. S.; de Souza, K. R.; Kwapinski, W.; Falcão, N. P. S.; Novotny, E. H.; Achete, C. A. Selective extraction of humic acids from an anthropogenic Amazonian dark earth and from a chemically oxidized charcoal. *Biol. Fertil. Soils* **2014**, *50*, 1223−1232.
(47) Zheng, J.; Liu, H.-T.; Wu, B.; Di, C.-A.; Guo, Y.-L.; Wu, T.; Yu, G.; Liu, Y.-Q.; Zhu, D.-B. Production of Graphite Chloride and Bromide Using Microwave Sparks. *Sci. Rep.* **2012**, *2*, 662.
(48) Watts, M.; Kosan, B.; Hammerschmidt, J.; Dorn, S.; Meister, F.; Scholl, S. Adsorptive Purification of Ionic Liquid and their Reuse in Cellulose Processing. *Chem. Ing. Tech.* **2017**, *89* (12), 1661−1668.
(49) Huang, K.; Wu, R.; Cao, Y.; Li, H.; Wang, J. Recycling and Reuse of Ionic Liquid in Homogeneous Cellulose Acetylation. *Chin. J. Chem. Eng.* **2013**, *21* (5), 577−584.
(50) Ren, S.; Hou, Y.; Wu, W.; Liu, W. Purification of Ionic Liquids: Sweeping Solvents by Nitrogen. *J. Chem. Eng. Data* **2010**, *55* (11), 5074−5077.
(51) Kono, H.; Hashimoto, H.; Shimizu, Y. NMR Characterization of Cellulose Acetate: Chemical Shift Assignments, Substituent Effects, and Chemical Shift Additivity. *Carbohydr. Polym.* **2015**, *118*, 91−100.
(52) Kim, C.-J.; Khan, W.; Kim, D.-H.; Cho, K.-S.; Park, S.-Y. Graphene Oxide/Cellulose Composite Using NMMO Monohydrate. *Carbohydr. Polym.* **2011**, *86*, 903−909.
(53) Kuzmenko, V.; Wang, N.; Haque, M.; Naboka, O.; Flygare, M.; Svensson, K.; Gatenholm, P.; Liu, J.; Enoksson, P. Cellulose-derived carbon nanofibers/graphene composite electrodes for powerful compact supercapacitors. *RSC Adv.* **2017**, *7* (73), 45968−45977.
(54) Cao, Y.; Wu, J.; Meng, T.; Zhang, J.; He, J.; Li, H.; Zhang, Y. Acetone-soluble Cellulose Acetates Prepared by One-step Homogeneous Acetylation of Cornhusk Cellulose in an Ionic Liquid 1-Allyl-3-methylimidazolium Chloride (AmimCl). *Carbohydr. Polym.* **2007**, *69*, 665−672.
(55) Wan Daud, W. R.; Djuned, F. M. Cellulose Acetate from Oil Palm Empty Fruit Bunch via a One Step Heterogeneous Acetylation. *Carbohydr. Polym.* **2015**, *132*, 252−260.
(56) Fan, X.; Liu, Z.-W.; Lu, J.; Liu, Z.-T. Cellulose Triacetate Optical Film Preparation from Ramie Fiber. *Ind. Eng. Chem. Res.* **2009**, *48* (13), 6212−6215.
(57) Mahmoudian, S.; Wahit, M. U.; Imran, M.; Ismail, A. F.; Balakrishnan, H. A Facile Approach to Prepare Regenerated Cellulose/Graphene Nanoplatelets Nanocomposite Using Room-Temperature Ionic Liquid. *J. Nanosci. Nanotechnol.* **2012**, *12* (7), 5233−5239.

https://dx.doi.org/10.1021/acs.biomac.9b01672
Biomacromolecules 2020, 21, 1752−1761